ORIGINAL PAPER

Improved square root cubature Kalman filter for state of charge estimation with state vector outliers

Zili Zhang[1] · Jing Chen[1] · Yawen Mao[1] · Cuicui Liao[1]

Abstract

In this paper, a square root cubature Kalman filter based multi-innovation least square (SRCKF-MILS) algorithm is proposed for state of charge (SOC) estimation. First, a second-order resistor-capacitor (RC) equivalent circuit model is constructed to approximate the dynamic performance of the battery. Then, the multi-innovation least square and the square root cubature Kalman filter are used to interactively estimate the battery model parameters and SOC. Since the state vector contains outliers, the strong tracking filtering (STF) theory is introduced to adaptively adjust the gain matrix. The STF theory combined with SRCKF-MILS algorithm can improve the robustness of the algorithm. Simulation examples show the effectiveness of the proposed algorithms.

Keywords State of charge · Multi-innovation least square algorithm · Second-order RC model · Strong tracking filter · Square root cubature Kalman filter

Introduction

Electric vehicles have been widely used due to their simple structure, little pollution and high energy efficiency [1–3]. As an important component of electric vehicles, lithium-ion batteries have attracted a lot of attentions [4, 5]. The properties of the battery are easily affected by temperature, voltage and current. It is essential to establish an effective battery management system (BMS) to maintain battery health [6–8]. The core factor of BMS is the SOC estimation, which reflects the performance of battery. Accurate SOC estimation can maximize battery performance [9, 10].

The nonlinear characteristics of battery system make the SOC estimation difficult. Recently, many algorithms have been proposed in the literature, including the current integration method, data-driven method, and adaptive filtering method [11–14]. For example, Wang et al. proposed an improved feedforward-long short-term memory (FF-LSTM) modeling method to realize an accurate whole-life-cycle SOC prediction by effectively considering the current, voltage, and temperature variations [15]. Jiao et al. proposed a gated recurrent unit recurrent neural network (GRU-RNN) based momentum gradient method to estimate SOC [16]. However, the data-driven method needs a large amount of training data, which involves heavy computational efforts. The adaptive filtering method considers the battery as a dynamic system and predicts SOC by constructing a state space model. In comparison to the other methods, it can improve estimation accuracy with little computational efforts [17–21].

The recursive least square (RLS) algorithm is a widely used online algorithm for lithium battery equivalent model [22–25]. Since only one set data are performed to update the estimates, the RLS algorithm has slow convergence rates [26–28]. In order to increase the convergence rates, Lao et al. [29] used the forgetting factor recursive least squares algorithm (FFRLS) to estimate unknown model parameters. However, as the number of iterations increases, the past data play less role on the parameter estimates. In [30], Ding

✉ Jing Chen
chenjing1981929@126.com

Zili Zhang
zhangzili1995@126.com

Yawen Mao
myw0530@163.com

Cuicui Liao
cliao@jiangnan.edu.cn

1 School of Science, Jiangnan University, Wuxi 214122, People's Republic of China

proposed a multi-innovation least square (MILS) algorithm, which expands the scalar innovation to vector innovation. Therefore, the MILS algorithm has faster convergence rates [31, 32].

Kalman filter (KF) is a powerful state estimation algorithm [33]. In the last few decades, some novel Kalman filters have been developed, such as the extended Kalman filter (EKF) [34], the unscented Kalman filter (UKF) [35], and the cubature Kalman filter (CKF) [36]. For high-dimensional nonlinear systems, the CKF has higher estimation accuracy and faster convergence rates [37, 38]. However, the covariance matrix does not remain positive definite, it may lead to the divergence of the filter. The square root cubature Kalman filter (SRCKF) algorithm can deal with this problem by performing recursive update in the form of the square root of the covariance matrix [39]. In applications, the state of lithium batteries is easily affected by environmental factors, which leads to outliers in the process noise matrix. To deal with this dilemma, Zhou proposed the strong tracking filter (STF) theory in [40], which makes the residual sequence orthogonal at each step. For this reason, the strong tracking filter theory combining the square root cubature Kalman filter can ensure the filter to track the system states, and has better robustness against model parameter mismatch.

In this paper, we propose two complementary cooperative algorithms for SOC estimation. The proposed square root cubature Kalman filter based multi-innovation least square (SRCKF-MILS) algorithm is used to estimate the battery model parameters and SOC interactively. The strong tracking square root cubature Kalman filter based multi-innovation least square (ST-SRCKF-MILS) algorithm can deal with state vector with outliers. The contributions of this study are summarized as follows.

1. Update SOC by the SRCKF-MILS algorithm, which can achieve more accurate SOC estimates than the HIf algorithm in [43].
2. Improve the SRCKF-MILS algorithm based on STF theory, which can deal with SOC with outliers.

The remaining part of this paper is organized as follows. In the "Online identification of battery model parameters" section, an online identification method of battery model parameters is introduced. In the "Estimating state of charge based on square root cubature Kalman filter" section, the SRCKF-MILS algorithm for SOC is proposed. In the "Improved square root cubature Kalman filter by strong tracking filter theory" section, the ST-SRCKF-MILS algorithm is studied. In the "Examples" section, two examples are provided. Finally, some conclusion remarks are given in the "Conclusions" section.

Online identification of battery model parameters

Battery model parameter estimation

In this paper, a second-order RC model is established to simulate battery charging and discharging behaviors. The basic structure is shown in Fig 1, where U represents the terminal voltage of the circuit, R_0 is the series resistance, R_1 is the polarization resistance, R_2 is the concentration polarization resistance, C_1 is the polarization capacitance, C_2 is the concentration polarization capacitance, U_{ocv} is the open circuit voltage, and I is the discharge current.

According to the Kirchhoff laws, the circuit equation can be described as follows:

$$\begin{cases} C_1 \frac{dU_1}{dt} = I(t) - \frac{U_1(t)}{R_1}, \\ C_2 \frac{dU_2}{dt} = I(t) - \frac{U_2(t)}{R_2}, \\ U = U_{ocv} - U_1 - U_2 - R_0 I(t). \end{cases} \tag{1}$$

Based on Laplace-transform method, we have

$$U_{ocv}(s) = \left(\frac{R_1}{R_1 C_1 s + 1} + \frac{R_2}{R_2 C_2 s + 1} + R_0 \right) I(s) + U(s). \tag{2}$$

Define $z(t) := U_{ocv}(t) - U(t)$, Eq. (2) can be transformed into

$$\begin{aligned} z(t) = &\ k_1 z(t-1) + k_2 z(t-2) + k_3 I(t) \\ &+ k_4 I(t-1) + k_5 I(t-2), \end{aligned} \tag{3}$$

where

$$\begin{cases} k_1 = \frac{8a-2}{1+2b+4a}, \\ k_2 = -\frac{1-2b+4a}{1+2b+4a}, \\ k_3 = -\frac{d+2c+4aR_0}{1+2b+4a}, \\ k_4 = -\frac{2d-8aR_0}{1+2b+4a}, \\ k_5 = -\frac{d-2c+4aR_0}{1+2b+4a}, \end{cases} \tag{4}$$
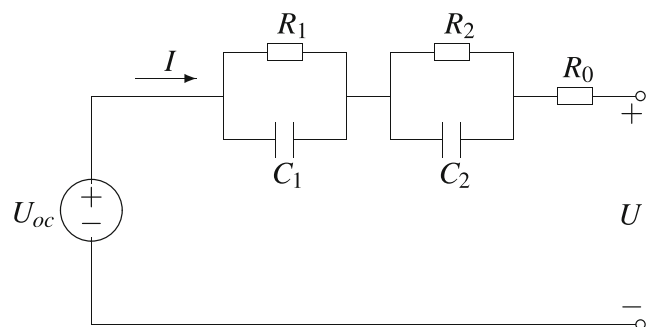

Fig. 1 Schematic diagram of the second-order RC model

and

$$\begin{cases} a = R_1 C_1 R_2 C_2, \\ b = R_1 C_1 + R_2 C_2, \\ c = R_1 R_2 C_2 + R_1 C_1 R_2 + R_0 (R_1 C_1 + R_2 C_2), \\ d = R_0 + R_1 + R_2. \end{cases} \quad (5)$$

The model is simplified as the following general linear model,

$$z(t) = \varphi^{\mathsf{T}}(t)\theta, \quad (6)$$

where $z(t)$ is system output, $\varphi(t) = [z(t-1), z(t-2), I(t), I(t-1), I(t-2)]^{\mathsf{T}}$ represents the information vector, and $\theta = [k_1, k_2, k_3, k_4, k_5]^{\mathsf{T}}$ denotes the unknown parameter vector.

Multi-innovation least squares algorithm

The RLS algorithm has several advantages, such as low memory occupation and high precision [30]. However, as the number of iterations increases, the past data have little ability to polish the system parameters. It leads to slow convergence rates. The MILS algorithm expands the information vector into an information matrix, the main steps are as follows:

$$\begin{aligned} \hat{\theta}(t) &= \hat{\theta}(t-1) + L(t) \left[Y(p, t) - \Phi^{\mathsf{T}}(p, t)\hat{\theta}(t-1) \right], \\ L(t) &= P(t-1)\Phi(p, t) \left[I_p + \Phi^{\mathsf{T}}(p, t)P(t-1)\Phi(p, t) \right]^{-1}, \\ P(t) &= P(t-1) - L(t)\Phi^{\mathsf{T}}(p, t)P(t-1), \\ \Phi(p, t) &= [\varphi(t), \varphi(t-1), \ldots, \varphi(t-p+1)], \\ Y(p, t) &= [y(t), y(t-1), \ldots, y(t-p+1)]^{\mathsf{T}}, \end{aligned}$$

where p is the innovation length.

The unknown parameters can be estimated by the MILS algorithm. The battery model parameters R_0, R_1, R_2, C_1, C_2 can be calculated using Eqs. (4) and (5). Since the output vector of the algorithm contains unmeasured parameter $U_{ocv}(t)$, it can be estimated by SRCKF.

Remark 1 When initializing $SOC(0)$, the corresponding $U_{ocv}(0)$ is obtained by the relationship between the U_{ocv}-SOC data, and in the subsequent iteration process, U_{ocv} is computed by the estimated SOC.

Remark 2 The relationship between the U_{ocv}-SOC data can be obtained through the pulse charge and discharge test. Due to the influence of battery hysteresis, the curves of the battery between charging and discharging are different. This paper takes their average curve as the real U_{ocv}-SOC relationship.

Estimating state of charge based on square root cubature Kalman filter

In this section, the battery state space model is constructed and the derivation of the SRCKF algorithm is presented.

Construction of the battery state space model

By integrating the charging and discharging current of the battery, the obtained integral value is the increase or decrease of the battery's charge. Assuming that the initial SOC of battery is $SOC(t_0)$, the SOC at the sampling time t_1 is written by

$$SOC(t_1) = SOC(t_0) - \frac{1}{C_E} \int_{t_0}^{t_1} \eta I(t) dt, \quad (7)$$

where $I(t)$ represents the battery's current, η is the Coulomb coefficient, and C_E indicates the rated capacity of the battery.

Remark 3 Equation (7) is the current integration method, which has a simple form to calculate SOC. The disadvantage of the current integration method is that if the current measurement is not accurate, the error will gradually accumulate, thus affecting the prediction results of the SOC. In this paper, Eq. (7) is used to construct a state space model to estimate SOC [18].

Combined with Eq. (1), the state space model of the battery is written as

$$\begin{cases} U_{1,k+1} = e^{-\frac{\Delta t_{k+1}}{R_1 C_1}} U_{1,k} + \left(1 - e^{-\frac{\Delta t_{k+1}}{R_1 C_1}} \right) R_1 I_k, \\ U_{2,k+1} = e^{-\frac{\Delta t_{k+1}}{R_2 C_2}} U_{2,k} + \left(1 - e^{-\frac{\Delta t_{k+1}}{R_2 C_2}} \right) R_2 I_k, \\ SOC_{k+1} = SOC_k - \frac{\eta t}{C_E} I_k, \\ U_k = F(SOC_k) - U_{1,k} - U_{2,k} - R_0 I_k. \end{cases} \quad (8)$$

Considering the noise term, Eq. (8) is transformed into

$$\begin{cases} x_{k+1} = A_k x_k + B_k U_k + Q_k, \\ y_k = F(SOC_k) - U_{1,k} - U_{2,k} - R_0 I_k + R_k, \end{cases} \quad (9)$$

where

$$\boldsymbol{x}_k = \begin{bmatrix} U_{1,k} \\ U_{2,k} \\ SOC_k \end{bmatrix}, \boldsymbol{A}_k = \begin{bmatrix} e^{-\frac{\Delta t_{k+1}}{R_1 C_1}} & 0 & 0 \\ 0 & e^{-\frac{\Delta t_{k+1}}{R_2 C_2}} & 0 \\ 0 & 0 & 1 \end{bmatrix},$$

$$\boldsymbol{B}_k = \begin{bmatrix} \left(1 - e^{-\frac{\Delta t_{k+1}}{R_1 C_1}}\right) R_1 \\ \left(1 - e^{-\frac{\Delta t_{k+1}}{R_2 C_2}}\right) R_2 \\ -\frac{\eta t}{C_E} \end{bmatrix}, \boldsymbol{U}_k = \begin{bmatrix} I_k \end{bmatrix}, \boldsymbol{Q}_k = \begin{bmatrix} Q_{1,k} \\ Q_{2,k} \\ Q_{3,k} \end{bmatrix}.$$

$F(x)$ is the functional relationship between SOC and U_{ocv}, $\boldsymbol{Q}_k$ and $\boldsymbol{R}_k$ represent process noise and measurement noise at time k, respectively.

Square root cubature Kalman filter

Since Eq. (9) contains the nonlinear function $F(x)$, the Kalman filter is unavailable for such a model. Here, an improved filtering method, termed as the cubature Kalman filter, is introduced.

Under the Gaussian approximation, the function recursion of the Bayesian filter is simplified to algebraic recursion, i.e., the mean and covariance of the conditional probability density function are calculated during time update and measurement update. It can be seen that the core of the filtering process is to calculate the Gaussian weight product of the integrand in the form of a nonlinear function and a Gaussian probability density function. Then, it follows that

$$I(p) = \int_D p(x)w(x)dx, \tag{10}$$

where $p(x)$ is a nonlinear function, $w(x) \geq 0$ is a weight function, $D \subseteq R^n$ indicates the integration area, $x = [x_1 \; x_2 \dots x_n] \in D$. The basic idea to solve this problem is to find a series of weighted points x_i with weight W_i for approximation,

$$I(p) \approx \sum_{i=1}^m W_i p(x_i). \tag{11}$$

Cubature rule is an effective method to determine these points. However, in the filtering process, the Cholesky factorization of the covariance matrix cannot guarantee its positive definiteness. The SRCKF algorithm can solve this problem by directly performing the recursive update in the form of the square root of the covariance matrix in the filtering process, and has the following advantages over the traditional CKF methods: (1) can reduce the computational complexity; (2) can ensure the positive definiteness of the covariance matrix; (3) can avoid the divergence of the filter; (4) can improve the convergence speed and numerical stability. In summary, the specific steps of the SRCKF are shown in Algorithm 1.

Require: Initialize the posterior error covariance matrix P_0, process noise and measurement noise Q_0, R_0, state vector $\hat{x}_0$

1: Decompose the posterior error covariance matrix:

$$\boldsymbol{P}_{k-1|k-1} = \boldsymbol{S}_{k-1|k-1} \boldsymbol{S}_{k-1|k-1}^{\mathrm{T}}. \tag{12}$$

2: Generate cubature points:

$$\boldsymbol{X}_{i,k-1|k-1} = \boldsymbol{S}_{k-1|k-1} \boldsymbol{\xi}_i + \hat{x}_{k-1|k-1}, i = 1, 2, \dots, m,$$

$$\boldsymbol{\xi}_i = \sqrt{\frac{m}{2}}[1]_i, \tag{13}$$

where n is the dimension of the state vector, $m = 2n$ is the number of cubature points, $[1]_i$ represents the i-th column of the following formula,

$$[1]_i = \begin{bmatrix} \begin{pmatrix} 1 \\ 0 \\ \vdots \\ 0 \end{pmatrix} \cdots \begin{pmatrix} 0 \\ 0 \\ \vdots \\ 1 \end{pmatrix} \begin{pmatrix} -1 \\ 0 \\ \vdots \\ 0 \end{pmatrix} \cdots \begin{pmatrix} 0 \\ 0 \\ \vdots \\ -1 \end{pmatrix} \end{bmatrix}.$$

3: Cubature point propagation:

$$\boldsymbol{X}_{i,k|k-1}^* = f(\boldsymbol{X}_{i,k-1|k-1}). \tag{14}$$

4: Predict the state vector:

$$\hat{x}_{k|k-1} = \frac{1}{m} \sum_{i=1}^m w_i \boldsymbol{X}_{i,k|k-1}^*. \tag{15}$$

5: Calculate the square root of the estimated error covariance matrix:

$$\boldsymbol{X}_{k|k-1}^* = \frac{1}{\sqrt{m}} \begin{bmatrix} \boldsymbol{X}_{1,k|k-1}^* - \hat{x}_{k|k-1} & \boldsymbol{X}_{2,k|k-1}^* - \hat{x}_{k|k-1} \\ \dots \boldsymbol{X}_{i,k|k-1}^* - \hat{x}_{k|k-1} \end{bmatrix}, \tag{16}$$

$$\boldsymbol{S}_{k|k-1} = \mathrm{qr}\left(\begin{bmatrix} \boldsymbol{X}_{k|k-1}^* & \sqrt{\boldsymbol{Q}_k} \end{bmatrix}\right). \tag{17}$$

6: Generate cubature points:

$$\boldsymbol{X}_{i,k|k-1} = \boldsymbol{S}_{k|k-1} \boldsymbol{\xi}_i + \hat{x}_{k|k-1}, i = 1, 2, \dots, m. \tag{18}$$

7: Cubature point propagation:

$$\boldsymbol{Z}_{i,k|k-1}^* = h(\boldsymbol{X}_{i,k|k-1}). \tag{19}$$

8: Predict the measured value:

$$\hat{z}_{k|k-1} = \frac{1}{m} \sum_{i=1}^m w_i \boldsymbol{Z}_{i,k|k-1}. \tag{20}$$

9: Calculate the square root of innovation covariance matrix:

$$\boldsymbol{\eta}_{k|k-1} = \frac{1}{\sqrt{m}} \begin{bmatrix} \boldsymbol{Z}_{1,k|k-1}^* - \hat{z}_{k|k-1} & \boldsymbol{Z}_{2,k|k-1}^* - \hat{z}_{k|k-1} \\ \dots \boldsymbol{Z}_{i,k|k-1}^* - \hat{z}_{k|k-1} \end{bmatrix}, \tag{21}$$

$$\boldsymbol{S}_{zz,k|k-1} = \mathrm{qr}\left(\begin{bmatrix} \boldsymbol{\eta}_{k|k-1} & \sqrt{\boldsymbol{R}_k} \end{bmatrix}\right). \tag{22}$$

Algorithm 1 The square root cubature Kalman filter algorithm.

10: Calculate the square root of cross-covariance matrix:

$$X_{k|k-1} = \frac{1}{\sqrt{m}}[X_{1,k|k-1} - \hat{x}_{k|k-1} \quad X_{2,k|k-1} - \hat{x}_{k|k-1}$$

$$\ldots X_{i,k|k-1} - \hat{x}_{k|k-1}], \tag{23}$$

$$P_{xz,k|k-1} = X_{k|k-1}\eta_{k|k-1}^{\mathsf{T}}. \tag{24}$$

11: Estimate Kalman gain:

$$K_k = \left(P_{xz,k|k-1}/S_{zz,k|k-1}^{\mathsf{T}}\right)/S_{zz,k|k-1}. \tag{25}$$

12: Compute the state vector:

$$\hat{x}_{k|k} = \hat{x}_{k|k-1} + K_k(z_k - \hat{z}_{k|k-1}). \tag{26}$$

13: Update the error covariance matrix:

$$S_{k|k} = \mathrm{qr}\left(\begin{bmatrix} X_{i,k|k-1} - K_k\eta_{k|k-1} & K_k\sqrt{R_k} \end{bmatrix}\right). \tag{27}$$

The SRCKF-MILS algorithm for SOC

This subsection introduces a complementary cooperative algorithm for estimating SOC. First, the MILS algorithm is used to estimate model parameters R_0, R_1, R_2, C_1 and C_2, which will be applied to estimate state vector (SOC is one of the states) by the SRCKF. Then, the open circuit voltage U_{ocv} can be obtained by the relationship between U_{ocv} and SOC. The whole process is updated interactively until the SOC is obtained.

The structure diagram of the algorithm is shown in Fig. 2, the relationship between the OCV and the SOC of the battery can be obtained by intermittent charge and discharge test as shown in Fig. 3.

Improved square root cubature Kalman filter by strong tracking filter theory

Strong tracking filter theory

As shown in Fig. 1, the second-order RC model can reflect the complex electrochemistry, such as polarization reaction and diffusion effect of lithium batteries. However, in applications, the states of lithium batteries change all the time, and are easily affected by environmental factors. This would lead to outliers in the process noise matrix. When using the SRCKF algorithm to estimate the state vector, the noise matrix containing outliers will seriously affect the estimation effect, and even cause the divergence of the filter. Combining the SRCKF algorithm with the STF theory can deal with this problem.

Lemma 1 [40] *A sufficient condition for a strong tracking filter is to choose an appropriate time-varying gain matrix such that:*

$$Condition1: \quad \mathrm{E}\left[x(k+1) - \hat{x}(k+1|k+1)\right]\left[x(k+1) - \hat{x}(k+1|k+1)\right]^{\mathsf{T}} = min, \tag{28}$$

$$Condition2: \quad \mathrm{E}\left[\varepsilon(k+1+j)\varepsilon^{\mathsf{T}}(k+1)\right] = 0,$$
$$k = 0, 1, 2, \ldots, j = 1, 2, \ldots \tag{29}$$

where ε is the output residual sequence $\varphi(x_k)$, $\varepsilon(k) = z(k) - \hat{z}(k|k-1)$.

Lemma 1 is the orthogonality lemma. Condition 1 is the performance index of Kalman filter, Condition 2 requires that the output residual sequences remain orthogonal. Due to the influence of model uncertainty, the state estimates of the filter may deviate from the real state. It is necessary to adjust the gain matrix K_k, to satisfy Eq. (29).

A time-varying factor λ_k is introduced to weaken the influence of the old data. The corresponding gain matrix can be obtained by adjusting the prediction error covariance matrix to satisfy the orthogonality theorem. The updated formula of the prediction error covariance matrix is:

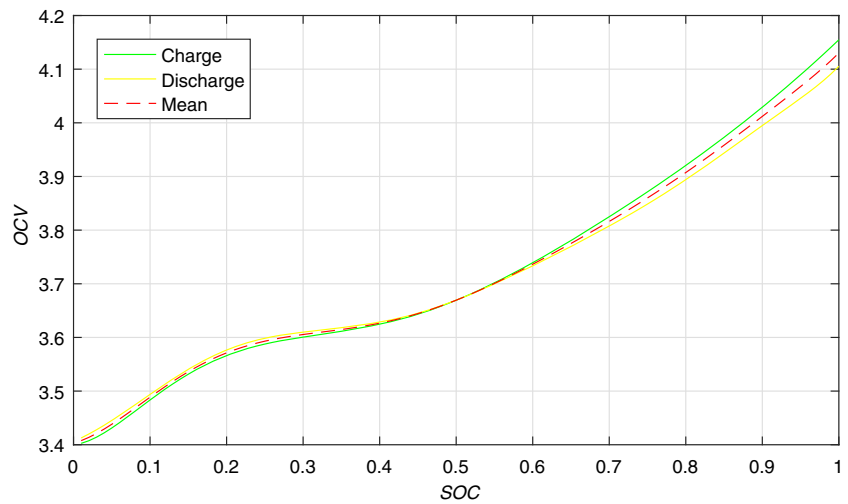$$P_{k|k-1} = F_k P_{k-1|k-1} F_k^{\mathsf{T}} + Q_k. \tag{30}$$

Adding the fading factor λ_k, the adjusted prediction error covariance matrix is written as follows:

$$P_{k|k-1} = \lambda_k F_k P_{k-1|k-1} F_k^{\mathsf{T}} + Q_k. \tag{31}$$

Fig. 2 Structure of SOC estimation strategy based on SRCKF-MILS
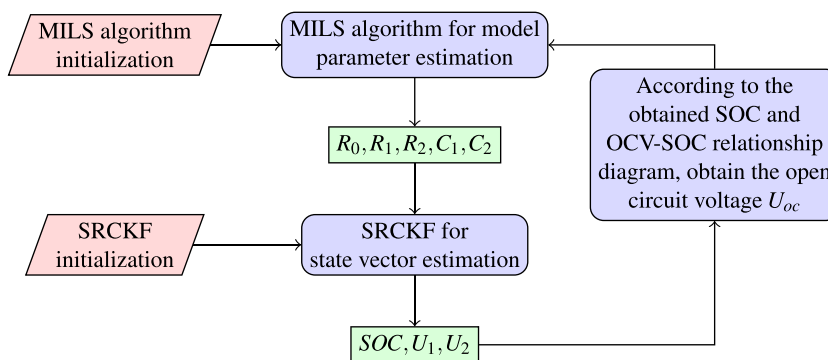
Fig. 3 Battery SOC-OCV average curve under intermittent charge and discharge test

Lemma 2 [41] *Let* $\Delta x(k) \triangleq x(k) - \hat{x}(k)$, $V_0(k+1) = E[\varepsilon(k+1)\varepsilon^{\mathsf{T}}(k+1)]$. *When* $O[|\Delta x(k)^2|] \ll O[|\Delta x(k)|]$, *the following equality holds,*

$$\mathrm{E}\left[\varepsilon(k+1+j)\varepsilon^{\mathsf{T}}(k+1)\right] \approx H(k+j+1) \cdot F(k+j)$$
$$[I - K(k+j)H(k+j)] \cdots F(k+2)[I - K(k+2)$$
$$H(k+2)] \cdot F(k+1)[P(k+1|k)H^{\mathsf{T}}(k+1) - $$
$$K(k+1)V_0(k+1)]. \tag{32}$$

It can be known from Lemma 2 that when the filter has ideal working performance, its output residual sequence is weakly autocorrelated. According to [40], define

$$S(k) = P(k+1|t)H^{\mathsf{T}}(k+1) - K(k+1)V_0(k+1). \tag{33}$$

The suboptimality of λ_{k+1} can be measured by minimizing the following performance indicator:

$$g(k+1) = \sum_{i=1}^{n}\sum_{j=1}^{m} s_{ij}^2, \tag{34}$$

where $S = (s_{ij})$. The specific steps are as follows [41]:

$$\lambda_k = \begin{cases} \lambda_k & \lambda_k \geq 1, \\ 1 & \lambda_k < 1, \end{cases} \tag{35}$$

where

$$\lambda_k = tr(N_k)/tr(M_k), \tag{36}$$
$$N_k = V_k - H_k Q_{k-1} H_k^{\mathsf{T}} - \beta R_k, \tag{37}$$
$$M_k = H_k F_k P_k F_k^{\mathsf{T}} H_k^{\mathsf{T}}, \tag{38}$$

$$V_k = \begin{cases} \varepsilon_1 \varepsilon_1^{\mathsf{T}} & k=1, \\ \\ \frac{\rho V_{k-1} + \varepsilon_k \varepsilon_k^{\mathsf{T}}}{1+\rho} & k>1, \end{cases} \tag{39}$$

where F_k is the linearization matrix of the state equation, H_k is the linearization matrix of the measurement equation,

$tr(\cdot)$ represents the trace of the matrix, ε_k is the output residual sequence, $\varepsilon_k = z_k - \hat{z}_{k|k-1}$, ρ is the forgetting factor, V_k is the covariance matrix of the residual sequence, and β is a weakening factor which can avoid over-regulation.

Strong tracking square root cubature Kalman filter

According to [42], the following equality holds,

$$H_k = (P_{xz,k|k-1})^{\mathsf{T}}(P_{k|k-1})^{-1}. \tag{40}$$

After introducing the suboptimal fading factor, assume that $P_{k|k-1}^e$, $P_{zz,k|k-1}^e$ and $P_{xz,k|k-1}^e$ represent the new prediction error covariance matrix, prediction output covariance matrix and cross-covariance matrix, respectively.

It is obvious that the following equalities hold,

$$P_{k|k-1}^e = F_k P_{k-1|k-1} F_k^{\mathsf{T}} + Q_k, \tag{41}$$
$$P_{zz,k|k-1}^e = H_k P_{zz,k-1|k-1} H_k^{\mathsf{T}} + R_k. \tag{42}$$
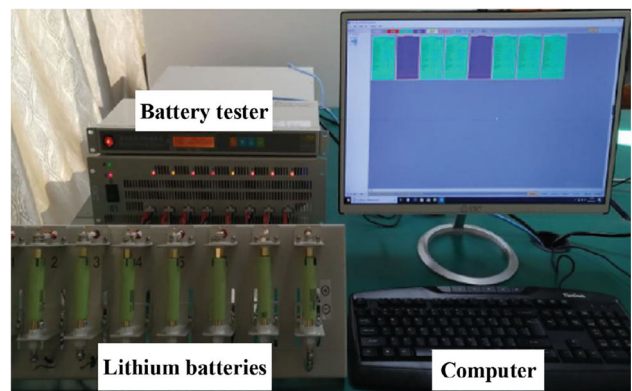
Fig. 4 The battery test platform

Table 1 The parameters of NCR18650PF

Capacity	2900 mAh
Normal voltage	3.63V
Min/max voltage	2.75V/4.2V
Standard charge/rapid charge	1.3A/2.6A
Max charge current	2.6A
Max discharge current	5.2A
Operating discharge temperature	$-20°C/60°C$
Dimensions	18.00*65.00mm

In the SRCKF algorithm, according to QR decomposition, the prediction error covariance matrix $\boldsymbol{P}_{k|k-1}$ and the prediction output covariance matrix $\boldsymbol{P}_{zz,k|k-1}$ can be obtained by updating the corresponding characteristic square roots $\boldsymbol{S}_{k|k-1}$ and $\boldsymbol{S}_{zz,k|k-1}$:

$$\boldsymbol{P}_{k|k-1} = \boldsymbol{S}_{k|k-1}\boldsymbol{S}_{k|k-1}^{\mathsf{T}}, \tag{43}$$

$$\boldsymbol{P}_{zz,k|k-1} = \boldsymbol{S}_{zz,k|k-1}\boldsymbol{S}_{zz,k|k-1}^{\mathsf{T}}. \tag{44}$$

In the same way, the following equation can be obtained:

$$\boldsymbol{P}_{k|k-1}^e = \boldsymbol{S}_{k|k-1}^e \left(\boldsymbol{S}_{k|k-1}^e\right)^{\mathsf{T}}, \tag{45}$$

$$\boldsymbol{P}_{zz,k|k-1}^e = \boldsymbol{S}_{zz,k|k-1}^e \left(\boldsymbol{S}_{zz,k|k-1}^e\right)^{\mathsf{T}}. \tag{46}$$

Therefore, when updating suboptimal fading factor λ_k, Eqs. (37) and (38) should be transformed into the following form:

$$\boldsymbol{N}_k = \boldsymbol{V}_k - \left(\boldsymbol{P}_{xz,k|k-1}^e\right)^{\mathsf{T}} \left(\boldsymbol{S}_{k|k-1}^e \left(\boldsymbol{S}_{k|k-1}^e\right)^{\mathsf{T}}\right)^{-1} \boldsymbol{Q}_{k-1}$$
$$\left(\boldsymbol{S}_{k|k-1}^e \left(\boldsymbol{S}_{k|k-1}^e\right)^{\mathsf{T}}\right)^{-1} \left(\boldsymbol{P}_{xz,k|k-1}^e\right)^{\mathsf{T}} - \beta \boldsymbol{R}_k, \quad (47)$$

$$\begin{aligned}
\boldsymbol{M}_k &= \boldsymbol{H}_k \boldsymbol{F}_k \boldsymbol{P}_{k|k} \boldsymbol{F}_k^{\mathsf{T}} \boldsymbol{H}_k^{\mathsf{T}}, \\
&= \boldsymbol{H}_k \left(\boldsymbol{P}_{k|k-1}^e - \boldsymbol{Q}_{k-1}\right) \boldsymbol{H}_k^{\mathsf{T}}, \\
&= \boldsymbol{P}_{zz,k|k-1}^e - \boldsymbol{R}_k - \boldsymbol{H}_k \boldsymbol{Q}_{k-1} \boldsymbol{H}_k^{\mathsf{T}}, \\
&= \boldsymbol{P}_{zz,k|k-1}^e + \boldsymbol{N}_k - \boldsymbol{V}_k + (\beta - 1)\boldsymbol{R}_k, \\
&= \boldsymbol{S}_{zz,k|k-1}^e \left(\boldsymbol{S}_{zz,k|k-1}^e\right)^{\mathsf{T}} \\
&\quad + \boldsymbol{N}_k - \boldsymbol{V}_k + (\beta - 1)\boldsymbol{R}_k. \tag{48}
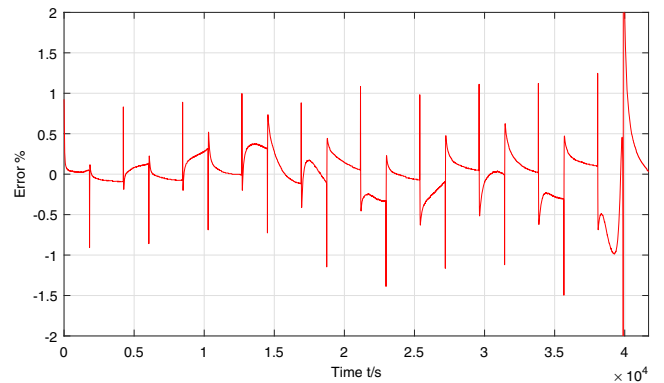\end{aligned}$$

The ST-SRCKF algorithm can be obtained by introducing the suboptimal fading factor. In Algorithm 1, Eq. (17) needs to be transformed into the following form:

$$S_{k|k-1} = \text{qr}\left(\left[\sqrt{\lambda_k}X_{i,k|k-1}^* \quad \sqrt{\boldsymbol{Q}_k}\right]\right). \tag{49}$$
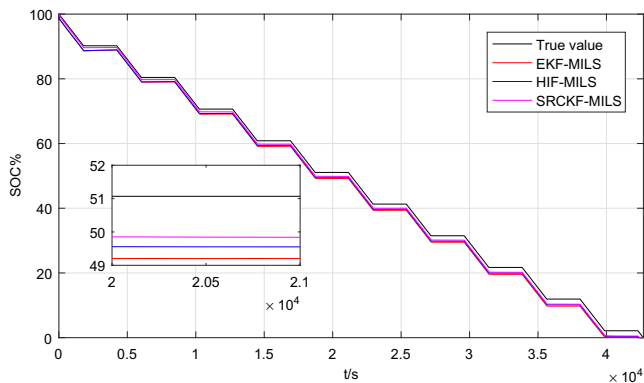
The steps of the ST-SRCKF algorithm are listed as follows.
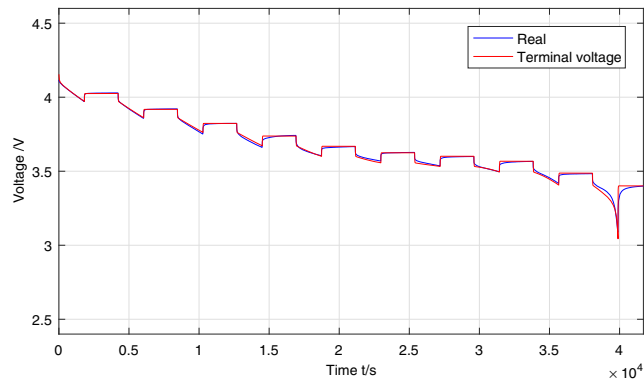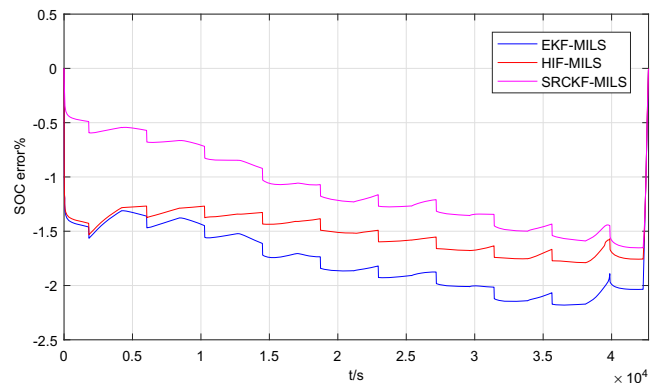

(a) Terminal voltage

(b) Terminal voltage errors

(c) SOC

(d) SOC errors

Fig. 5 The errors of SOC estimation under intermittent discharge test

Table 2 Estimation errors of SOC

Algorithm	EKF-MILS	HIf-MILS	SRCKF-MILS
MAE	1.7796	1.5182	1.1109
RMSE	1.3340	1.2321	1.0540

1. Initialize the posterior error covariance matrix $\boldsymbol{P}_0$, process noise $\boldsymbol{Q}_0$ and measurement noise $\boldsymbol{R}_0$, state vector $\hat{\boldsymbol{x}}_0$, and let $k=1$.
2. Predict the state vector $\hat{x}_{k|k-1}$ by Eqs. (13)–(24) in Algorithm 1.
3. Calculate suboptimal fading factor λ_k by Eqs. (35), (36), (39), (47), (48).
4. Update the prediction error covariance matrix $\boldsymbol{S}_{k|k-1}$ using Eq. (49).
5. Update the output error covariance matrix $\boldsymbol{S}_{zx,k|k-1}$ and the cross-covariance matrix $\boldsymbol{P}_{zx,k|k-1}$ by Eqs. (18)–(24) in Algorithm 1.
6. Update the state vector $\hat{x}_{k|k}$ by Eqs. (25)–(27) in Algorithm 1.
7. If $||\hat{x}_{k|k} - \hat{x}_{k-1|k-1}|| \leq \varepsilon$, obtain the $\hat{x}_{k|k}$. Otherwise, increase k by 1 and go to step 2.
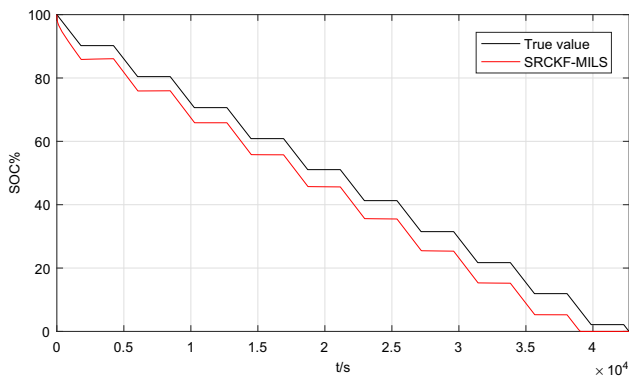
Examples

The battery tester platform

Referring to Fig. 4, the battery experiment platform is used to detect the Li(NiCoMn)O2 material lithium-ion battery cell, and the experiment is carried out at room temperature 25°C. The battery experiment platform includes a battery tester (NEWARE CT-4008-5V12A), a battery holder, Samsung ICR18650 (2600 mAh) lithium-ion batteries, and a host computer. The main parameters of the lithium-ion battery are shown in Table 1.

Simulation process

Two simulation examples are given to verify the effectiveness of the SRCKF-MILS algorithm and the ST-SRCKF-MILS algorithm.

Apply the EKF-MILS algorithm, the HIf-MILS algorithm and the SRCKF-MILS algorithm to estimate SOC, respectively. The terminal voltage estimation is shown in Fig. 5(a). The terminal voltage estimation errors are shown in Fig. 5(b). Figure 5(c) shows the SOC estimation by different algorithms, and Fig. 5(d) shows the SOC estimation
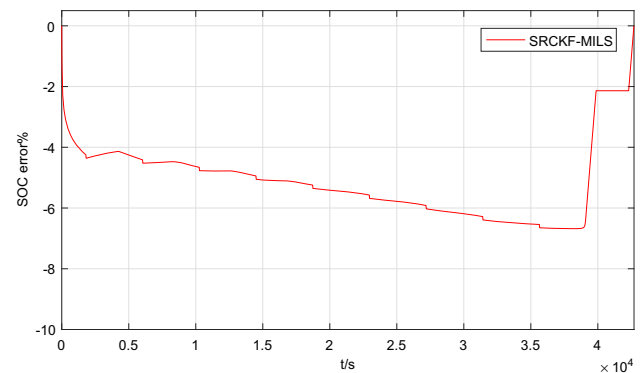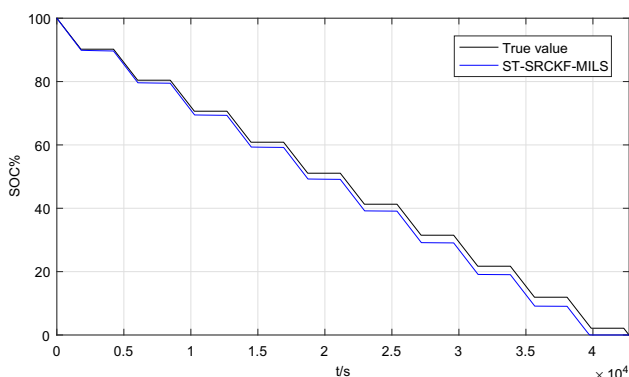
(a) SOC with state vector outliers by SRCKF-MILS

(b) SOC errors with state vector outliers by SRCKF-MILS

(c) SOC with state vector outliers by ST-SRCKF-MILS
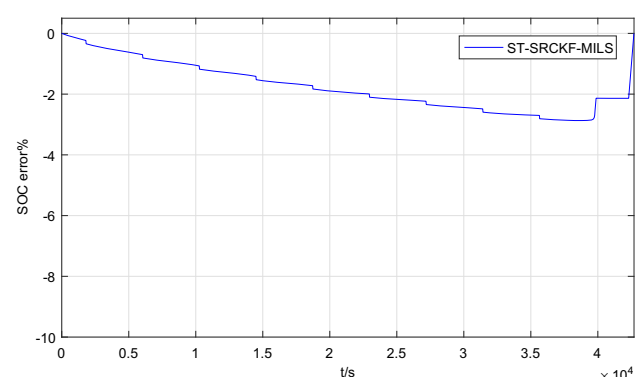
(d) SOC errors with state vector outliers by ST-SRCKF-MILS

Fig. 6 SOC estimation with state vector outliers

Table 3 Estimation errors of SOC with state vector outliers

Algorithm	ST-SRCKF-MILS	SRCKF-MILS
MAE	1.7612	5.1169
RMSE	1.3271	3.1623

errors. The MAE and RMSE of those algorithms are shown in Table 2.

In order to verify the robustness of the system state, a strong disturbance is artificially added in the iterative process to simulate the outliers of the state vector.

In the first experiment, take the number of iterations as 200~400, and change the state of the system to a value that deviates from the mean by more than two times of the standard deviations. Figure 6(a) and (b) depict the estimated values and errors of the SRCKF-MILS algorithm, respectively. Figure 6(c) and (d) show the estimated values and errors of the ST-SRCKF-MILS algorithm, respectively. The MAE and RMSE of the SRCKF-MILS algorithm and the ST-SRCKF-MILS algorithm are shown in Table 3.

In the second experiment, change the state of the system to a value that deviates from the mean by more

than three times of the standard deviations. Figure 7(a) and (b) show the estimated values and errors of the SRCKF-MILS algorithm, respectively. Figure 7(c) and (d) depict the estimated values and errors of the ST-SRCKF-MILS algorithm, respectively. The MAE and RMSE of the SRCKF-MILS algorithm and the ST-SRCKF-MILS algorithm are shown in Table 4.

Ultimately, numerical simulation suggests the following findings:

1. Table 2, Fig. 5(c) and (d) show that the SRCKF-MILS algorithm has the highest estimation accuracy than the EKF-MILS algorithm and the HIf-MILS algorithm.
2. Figure 6 shows that the ST-SRCKF-MILS algorithm is more stable and has smaller estimation errors than the SRCKF-MILS algorithm when the system has state vector outliers.
3. Figure 7 shows that the SRCKF-MILS algorithm diverges when the system has more serious outliers. For the ST-SRCKF-MILS algorithm, although the estimation errors become larger and larger, it remains stable and has a good performance. It illustrates that the ST-SRCKF-MILS algorithm has better robustness.
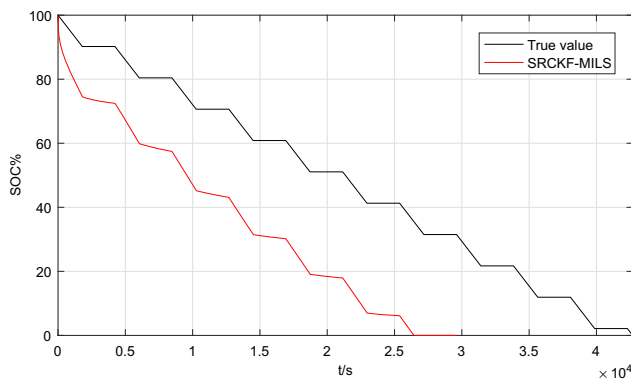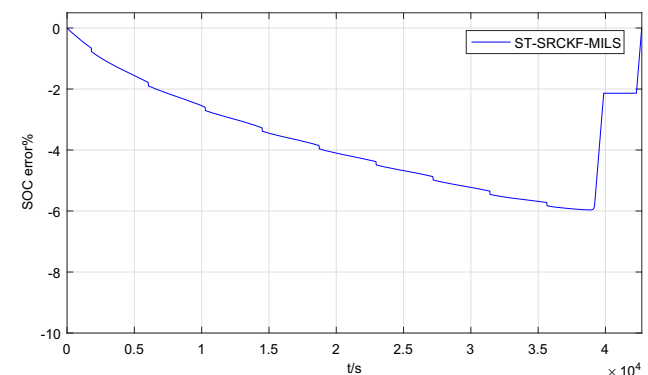

(a) SOC with state vector serious outliers by SRCKF- MILS
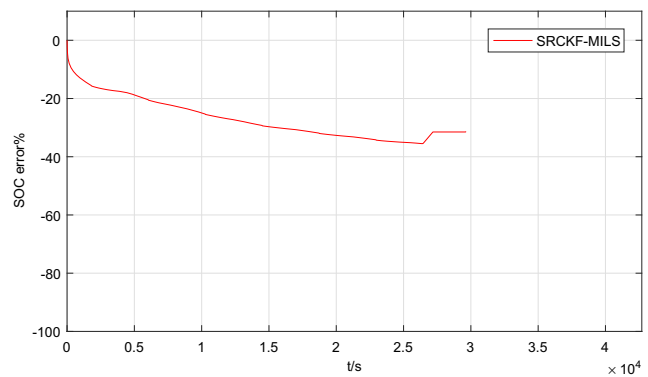
(b) SOC errors with state vector serious outliers by SRCKF-MILS
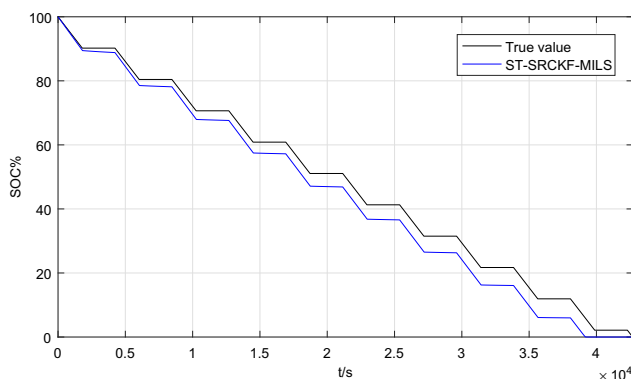
(c) SOC with state vector serious outliers by ST-SRCKF-MILS

(d) SOC errors with state vector serious outliers by ST-SRCKF-MILS

Fig. 7 SOC estimation with state vector serious outliers

Table 4 Estimation errors of SOC with state vector serious outliers

Algorithm	ST-SRCKF-MILS	SRCKF-MILS
MAE	3.6509	NAN
RMSE	1.9107	NAN

Conclusions

For the lithium batteries, two complementary cooperative algorithms are proposed to estimate SOC. The first one is the SRCKF-MILS algorithm, which estimates SOC interactively by the MILS algorithm and the SRCKF algorithm. Compared with the classical EKF algorithm and the HIf algorithm in [43], the proposed method improves the accuracy of estimates. In view of the existence of outliers in the state vector, an ST-SRCKF-MILS algorithm is further proposed. Simulation experiments show that the ST-SRCKF-MILS algorithm has better robustness. In addition, the proposed methods can be extended to life prediction for super-capacitors, and can be applied to model block-oriented dynamic systems.

References

1. Duan XY, Hu ZC, Song YH, Strunz K, Cui Y, Liu LK (2022) Planning strategy for an electric vehicle fast charging service provider in a competitive environment. IEEE Transactions on Transportation Electrification. https://doi.org/10.1109/TTE.2022.3152387

2. Sraidi S, Maaroufi M (2021) Study of electric vehicle charging impact. Lect Notes Netw Syst 216:427–437

3. Yadlapalli RT, Kotapati A, Kandipati R, Koritala CS (2022) A review on energy efficient technologies for electric vehicle applications. J Energy Storage 50:104212

4. Sashmitha K, Rani MU (2022) A comprehensive review of polymer electrolyte for lithium-ion battery. Polymer Bulletin. https://doi.org/10.1007/s00289-021-04008-x

5. Preger Y, Loraine TC, Rauhala T, Jeevarajan J (2022) Perspective on the safety of aged Lithium-ion batteries. J Electrochem Soc 169(3):030507

6. Belaid S, Rekioua D, Oubelaid A, Ziane D, Rekioua T (2022) A power management control and optimization of a wind turbine with battery storage system. J Energy Storage 45:103613

7. Liu ZJ, Qiu HF, Weng LG, Luo M, Wang X, Wang Q, Zhang D (2022) Facile synthesis of nitrogen deficient-carbon nitride as an efficient polysulfide barrier for lithium-sulfur battery. Ionics. https://doi.org/10.1007/s11581-022-04781-3

8. Kim T, Ochoa J, Faika T, Mantooth HA, Di J, Li QH, Lee Y (2020) An overview of cyber-physical security of Battery management systems and adoption of Blockchain technology. IEEE J Emerg Sel Top Power Electron 10(1):1270–1281

9. Jiao M, Wang DQ, Qiu J (2021) More intelligent and robust estimation of battery state-of-charge with an improved regularized extreme learning machine. Eng Appl Artif Intel 104:104407

10. Jiao M, Yang Y, Wang DQ, Gong P (2021) The conjugate gradient optimized regularized extreme learning machine for estimating state of charge. Ionics 27(11):4839–4848

11. Hossain LMS, Hannan MA, Hussain A, Hoque MM, Pin KJ, Saad MHM, Ayob A (2018) A review of state of health and remaining useful life estimation methods for lithium-ion battery in electric vehicles: Challenges and recommendations. J Clean Prod 205:115–133

12. Wang SL, Fernandez C, Yu CM, Fan YC, Cao W, Stroe DI (2020) A novel charged state prediction method of the lithium ion battery packs based on the composite equivalent modeling and improved splice Kalman filtering algorithm. J Power Sources 471:1–13

13. Wang SL, Ren P, Paul TA, Jin SY, Fernandez C (2022) A critical review of improved deep convolutional neural network for multi-timescale state prediction of Lithium-ion batteries. Energies 15(14):5053

14. Wang SL, Fan YC, Jin SY, Paul TA, Fernandez C (2023) Improved anti-noise adaptive long short-term memory neural network modeling for the robust remaining useful life prediction of Lithium-ion batteries. Reliab Eng Syst Saf 230. https://doi.org/10.1016/j.ress.2022.108920

15. Wang SL, Paul TA, Jin SY, Yu CM, Fernandez C, Stroe DI (2022) An improved feedforward-long short-term memory modeling method for the whole-life-cycle state of charge prediction of lithium-ion batteries considering current-voltage-temperature variation. Energy 254:124224

16. Jiao M, Wang DQ, Qiu J (2020) A GRU-RNN based momentum optimized algorithm for SOC estimation. J Power Sources 459:228051

17. Cho BH, Kim J, Shin J, Chun C (2011) Stable configuration of a li-ion series battery pack based on a screening process for improved voltage/SOC balancing. IEEE Trans Power Electron 27(1):411–424

18. Andre D, Nuhic A, Guth TS (2013) Comparative study of a structured neural network and an extended Kalman filter for state of health determination of lithium-ion batteries in hybrid electricvehicles. Eng Appl Artif Intel 26(3):951–961

19. Xia BZ, Sun Z, Zhang RF, Lao ZZ (2017) A cubature particle filter algorithm to estimate the state of the charge of Lithium-ion batteries based on a second-order equivalent circuit model. Energies 10(4):1–15

20. Wen LZ, Wang L, Guan ZW, Liu XM, Wei MJ, Jiang DH, Zhang SX (2022) Effect of composite conductive agent on internal resistance and performance of lithium iron phosphate batteries. Ionics. https://doi.org/10.1007/s11581-022-04491-w

21. Seongjun L, Jonghoon K, Jaemoon L, Cho BH (2008) State-of-charge and capacity estimation of lithium-ion battery using a new open-circuit voltage versus state-of-charge. J Power Sources 185(2):1367–1373

22. Patat S, Rahman S, Dokan FK (2022) The effect of sodium and niobium co-doping on electrochemical performance of $Li_4Ti_5O_{12}$ as anode material for lithium-ion batteries. Ionics. https://doi.org/10.1007/s11581-022-04579-3

23. Gan M, Chen XX, Ding F, Chen GY, Chen CLP (2019) Adaptive RBF-AR models based on multi-innovation least squares method. IEEE Sig Process Lett 26(8):1182–1186

24. Wang DQ, Fan QH, Ma Y (2020) An interactive maximum likelihood estimation method for multivariable Hammerstein systems. J Frankl Inst 357(17):12986–13005

25. Wang DQ, Zhang Z, Yuan JY (2017) Maximum likelihood estimation method for dual-rate Hammerstein systems. Int J Control Autom Syst 15(2):698–705

26. Ding F, Ma H, Pan J, Yang EF (2020) Hierarchical gradient and least squares based iterative algorithms for input nonlinear output-error systems using the key term separation. J Frankl Inst 358(9):5113–5135

27. Ding F, Zhang X, Xu L (2019) The innovation algorithms for multivariable state-space models. Int J Adapt Control Sig Process 33(11):1601–1608

28. Ayatinia M, Forouzanfar M, Ramezani A (2022) An LMI approach to robust iterative learning control for linear discrete-time systems. International Journal of Control, Automation and Systems. https://doi.org/10.1007/s12555-021-0429-x

29. Lao Z, Xia B, Wang W, Sun W, Lai Y, Wang M (2018) A novel method for lithium-ion battery online parameter identification based on variable forgetting factor recursive least squares. Energies 11(6):1358

30. Ding F, Chen T (2007) Performance analysis of multi-innovation gradient type identification methods. Automatica 43(1):1–14

31. Wang DQ, Yan YR, Liu YJ, Ding JH (2019) Model recovery for Hammerstein systems using the hierarchical orthogonal matching pursuit method. J Comput Appl Math 345:135–145

32. Wang DQ, Li LW, Ji Y, Yan YR (2018) Model recovery for Hammerstein systems using the auxiliary model based orthogonal matching pursuit method. Appl Math Model 54:537–550

33. Kalman RE (1960) A new approach to linear filtering and prediction problems. J Fluids Eng 82(1):35–45

34. Middleton R, Freeston M, McNeill L (2004) An application of the extended Kalman filter to robot soccer localisation and world modelling. IFAC Proc Vol 37(14):729–734

35. Cai Z, Zhao D (2006) Unscented Kalman filter for non-linear estimation. Geomatics Inf Sci Wuhan Univ 31(2):180–1083

36. Arasaratnam I, Haykin S (2009) Cubature Kalman filter. IEEE Trans Autom Control 54(6):1254–1269

37. Zheng YJ, Cui YF, Han XB, Dai HF, Ouyang MG (2021) Lithium-ion battery capacity estimation based on open circuit voltage identification using the iteratively reweighted least squares at different aging levels. J Energy Storage 44:103487

38. Ling L, Sun DM, Yu XL, Huang R (2021) State of charge estimation of lithium-ion batteries based on the probabilistic fusion of two kinds of cubature Kalman filters. J Energy Storage 43:103070

39. Zhang A, Bao SD, Bi WH, Yuan Y (2016) Low-cost adaptive square-root cubature Kalman filter for systems with process model uncertainty. J Syst Eng Electron 27(5):945–953

40. Zhou DH, Xi YG, Zhang ZJ (1900) Subopcimal fading extended Kalman filtering for nonlinear systems. Control Decis 5(5):1–6

41. Zhou DH, Xi YG, Zhang ZJ (1991) A suboptimal multiple fading extended Kalman Filter. Chin J Autom 4(2):145–152

42. Wang XX, Zhang L, Xia QX (2010) Strong tracking filter based on unscented transformation. Control Decis 25(7):1063–1068

43. Yao JX, Ding J, Cheng YY, Feng L (2021) Sliding mode-based H-infinity filter for SOC estimation of lithium-ion batteries. Ionics 27(12):5147–5157